

# Wavelength Add-Drop Switching Using Tilting Micromirrors

Joseph E. Ford, Vladimir A. Aksyuk, David J. Bishop, and James A. Walker

**Abstract**—This paper describes a single-mode optical fiber switch which routes individual signals into and out of a wavelength multiplexed data stream without interrupting the remaining channels. The switch uses free-space optical wavelength multiplexing and a column of micromechanical tilt-mirrors to switch 16 channels at 200 GHz spacing from 1531 to 1556 nm. The electrostatically actuated tilt mirrors use an 80 V peak-to-peak 300 KHz sinusoidal drive signal to switch between  $\pm 10^\circ$  with a 20  $\mu$ s response. The total fiber-to-fiber insertion loss for the packaged switch is 5 dB for the passed signals and 8 dB for added and dropped signals, with 0.2 dB polarization dependence. Switching contrast was 30 dB or more for all 16 channels and all input and output states. We demonstrate operation by switching 622 Mb/s data on eight wavelength channels between the two input and output ports with negligible eye closure.

**Index Terms**—Gratings, microelectromechanical devices, optical communications, optical fiber switches, wavelength division multiplexing (WDM).

## I. INTRODUCTION

CONVERTING fiber transmission systems from single wavelength to wavelength division multiplexing (WDM) provides inexpensive bandwidth but can sacrifice routing flexibility, because diverting part of the traffic in a simple WDM line system to an intermediate destination requires that all of the remaining wavelength signals must be detected and regenerated. As the number of wavelengths increases to 40 or more, the cost of providing dense WDM repeaters on the transmitted channels becomes prohibitive. These repeaters can be eliminated using wavelength add-drop: a transparent optical component to divert selected wavelength signals out of a WDM transmission line and also add new signals to reuse the dropped wavelengths [1]. Fixed wavelength add-drop (WAD) on a moderate number of channels can be accomplished with a set of notch filters [2]. But fully reconfigurable (electrically controlled) WAD allows efficient bandwidth allocation and fault recovery. Efficient, high-contrast WAD switching has become a high priority, especially for metropolitan networks. Reconfigurable WAD switches can be assembled from discrete wavelength multiplexers and switches (e.g., connecting microoptomechanical  $1 \times 1$  switches to arrayed waveguide routers [3]) or using an optical circulator with reflective fiber grating notch filters tuned by either temperature [4] or

magnetic field [5]. Planar waveguide switches have also been integrated with the router onto a single substrate, either as separate  $2 \times 2$  switches [6] or using two waveguide grating routers connected by waveguides containing phase-shifters [7].

Mechanical switches based on macroscopic bulk optics and electromechanical actuators have the best insertion loss and crosstalk performance of any switch technology, but are larger, slower, and potentially less reliable than solid-state switches. Micromechanical switches may achieve the same high performance levels of bulk optics, yet provide the compactness and reliability of solid state devices. In this paper, we demonstrate WAD using surface-normal operation of microoptomechanical switch arrays with free-space optical interconnection to single mode fiber inputs and outputs [8]. We describe the design of the wavelength multiplexing optics and the micromechanical switches, present monochromatic and broad spectrum measurements on the WAD switch, then conclude with some comments on the ultimate potential of this approach.

## II. SWITCH DESIGN

The block diagram for our WAD switch (Fig. 1) shows the four WDM fiber ports; IN, PASS, ADD, and DROP. The main input is connected through an optical circulator to a wavelength demultiplexer and then to a set of individual  $1 \times 1$  switches, each of which can reflect or transmit one wavelength channel. Reflected signals retrace their path through the wavelength multiplexer and into the circulator, which separates the back-reflected light into the PASS output. Transmitted signals are collected by a separate wavelength multiplexer and directed into the second port of a second optical circulator to the DROP output. The ADD port, connected to the first input of the second optical circulator, brings in the new data by retracing the same optical path created by dropping the input channels. In essence, the WAD creates an individual  $2 \times 2$  switch for each wavelength channel where the two allowed states are IN to PASS, or IN to DROP and ADD to PASS. Data is never routed from ADD to DROP. In this switch design, wavelength multiplexing of the added and dropped channels, if necessary, is done by an external router. Our implementation of this design connects two circulators [9] to a separate optomechanical package with the free-space wavelength multiplexing and micromechanical switch array.

Microelectromechanical systems (MEMS) is a device technology using lithographic fabrication techniques developed for silicon electronics to create miniature mechanical components. Elements are partially released from the substrate using a

Manuscript received December 29, 1998; revised February 11, 1999.  
J. E. Ford and J. A. Walker are with Bell Laboratories Lucent Technologies, Holmdel, NJ 07733 USA.

V. A. Aksyuk and D. J. Bishop are with Bell Laboratories Lucent Technologies, Murray Hill, NJ 07974 USA.

Publisher Item Identifier S 0733-8724(99)03799-8.

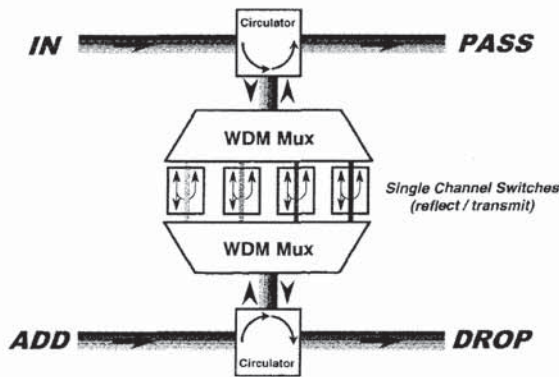


Fig. 1. Wavelength add-drop switch configuration.

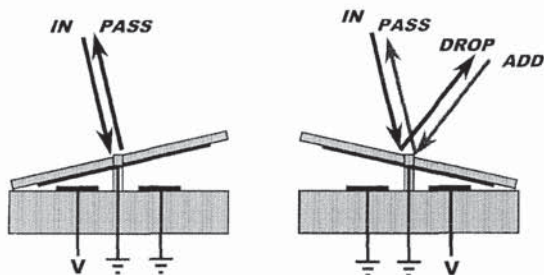


Fig. 2. Tilting micromirror switch geometry.

selective etch to remove portions of one or more sacrificial films. This produces structures which are mechanically active yet partially constrained (attached) to the surface [10]. One of the earliest commercial MEMS actuators was a display using a two-dimensional (2-D) array of tilting micromirrors a display developed by Texas Instruments using [11]. These components are now driving commercial  $800 \times 600$  pixel projection displays, demonstrating that high yield and reliability can be achieved with 480 000 element micromechanical device arrays.

Fig. 2 shows the geometry used in our WAD switch. An input signal is imaged onto the tilt mirror so that in one switch state (PASS) the signal is back reflected and in the other state (DROP) the signal is tilted to reflect the input toward the “add” signal source, so that the original input and add signals are counter-propagating. The switch is never required to route light from the ADD to DROP ports. If a switch element set to PASS is illuminated from the “add” source, the reflected light beam is tilted away from both PASS and DROP ports (a path not shown in the diagram). To complete the WAD, each element in a linear array of such switches is illuminated by a single wavelength picked out of the WDM fiber transmission.

#### A. Free-Space Wavelength Multiplexing

The wavelength multiplexing optics used in this switch were originally designed for a micromechanical spectral equalizer [12], where a continuous variable-reflectivity mirror illuminated by a wavelength-dispersed signal enabled dynamic

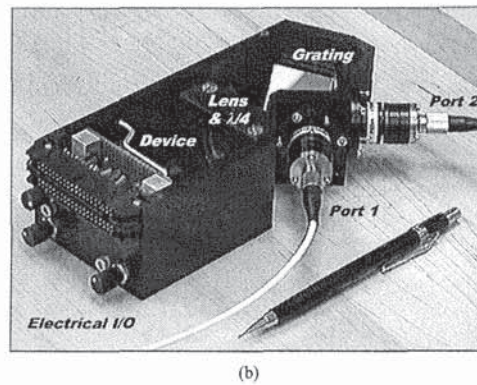
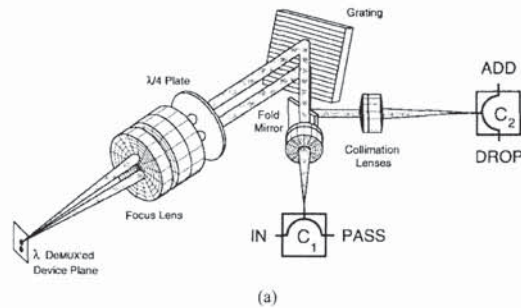


Fig. 3. (a) Free-space wavelength multiplexing optics layout and (b) optomechanical package.

power equalization. Fig. 3(a) shows the optical system layout. Light from an input fiber is collimated by a 25 mm focal length doublet lens and illuminates a 600 lines/mm diffraction grating blazed at a  $34^\circ$  angle. The diffracted signal is focused by a 50 mm focal length triplet lens onto the device plane, where the broad spectrum input is distributed over a device array. The system uses pupil division to separate the input and reflected output signals. The focus lens is shifted down relative to the input illumination, so that the collimated input beam illuminates the top half of the lens, and the light reflected from the device array illuminates the bottom half of the lens. The reflected signal diffracts from a second pass off the grating, which recombines the spectral components. A small fold mirror positioned below the main optical axis picks off the reflected signal and directs it into an output collimator which focuses the signal into a second optical fiber.

The grating diffraction efficiency has some polarization dependence. The insertion loss at 1543 nm ranges from about 0.6 to 1.1 dB. If uncorrected, the double-passed grating would produce 1 dB or more of polarization dependent loss (PDL). However, PDL can be suppressed using a quarter wave plate oriented at  $45^\circ$  to the grating lines so that the reflected signal is rotated by  $90^\circ$  before the second pass through the grating. This way, any input polarization is attenuated by twice the average insertion loss of the grating (1.7 dB for the current grating).

Fig. 3(b) shows the connectorized opto-mechanical package, including electrical connections for device control and a number of tip/tilt/translation controls for optical alignment.

The total fiber-to-fiber insertion loss for this package, measured using a simple gold mirror at the device plane, is 4.6 dB, with 0.2 dB PDL. This package is intended for laboratory environments. However, once the mechanics are aligned and locked down, the package can be handled and fibers can be attached and removed with minimal (<0.5 dB) change in insertion loss.

For operation as a switch, the device array must be designed so that the two mirror states either back reflect the input into the first collimating lens or tilt the beam toward the second collimator. Reflections from the fiber to free-space transition must also be suppressed, so antireflection coated and angle-polished FC connectors were used on fibers fusion-spliced directly to the circulators.

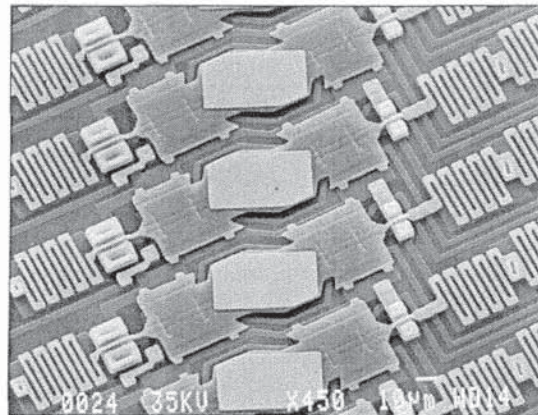
### B. Micromechanical Tilt-Mirror Switch

The tilt-mirror switch geometry is dictated by the beam path through the optical system. The basic requirement to switch from a transmissive to a reflective WDM path is to place a flat mirror at the location of each monochromatic signal in the device plane and reflect the incident cone of light back toward the focus lens so that it either overlaps the original input beam area (in the PASS state), or is shifted to the lower half of the focus lens and imaged to the second optical fiber output (in the DROP state). Given the numerical aperture of the single mode fiber source (about 0.2) and the magnification of the imaging between fibers and device plane (two times), the full tilt angle required to avoid overlap between the two switch states is at least  $6^\circ$ . With a 200 GHz (1.59 nm) WDM signal spacing, the mirrors must match a  $57\text{ }\mu\text{m}$  pitch of the signals at the device plane.

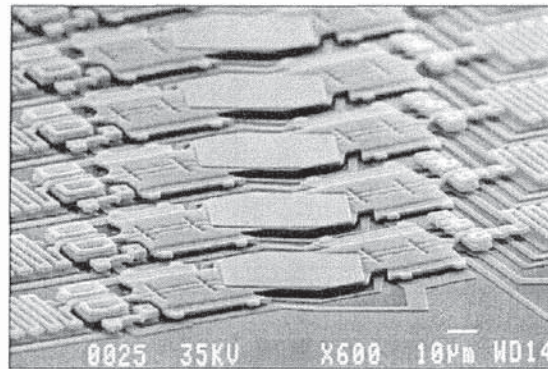
The devices used in this demonstration were fabricated through the multiuser MEMS processes (MUMP's) commercial MEMS foundry operated by the Microelectronics Center of North Carolina (MCNC).<sup>1</sup> MUMP's is a general purpose three-layer polysilicon surface micromachining process using polysilicon as the structural material, deposited oxide (phosphosilicate glass, PSG) as the sacrificial material, silicon nitride for electrical isolation from the substrate, and a top layer of metal. The layer structure, from the bottom up, is: silicon substrate,  $0.6\text{ }\mu\text{m}$  of nitride,  $0.5\text{ }\mu\text{m}$  of polysilicon,  $2\text{ }\mu\text{m}$  of PSG,  $2\text{ }\mu\text{m}$  of polysilicon,  $0.75\text{ }\mu\text{m}$  of PSG,  $1.5\text{ }\mu\text{m}$  of polysilicon, and  $0.5\text{ }\mu\text{m}$  of metal (gold, with a thin chrome adhesion layer). In our devices, the moving mirror switch is made from the top  $1.5\text{ }\mu\text{m}$  thick polysilicon and the  $0.5\text{ }\mu\text{m}$  metal layers.

Fig. 4(a) and (b) shows two SEM micrographs of the fabricated switch, with a gold-coated polysilicon tilt-mirror suspended  $2.75\text{ }\mu\text{m}$  above the silicon substrate. The mirror area is  $30 \times 50$  microns, with a  $57\text{-}\mu\text{m}$  pitch between the 16 devices. The photographs reveal a  $24^\circ$  angle between the mirror tilt axis and the column of devices. This comes from matching the skew-ray beam path through the focus lens to exactly overlap the input and output beams. The mirrors are supported

<sup>1</sup>MCNC's MEMS Technology Applications Center was recently separated as an independent commercial entity called Cronos Integrated Microsystems Incorporated. For more information, see HYPERLINK <http://mems.mcnc.org/mumps.html>; <http://mems.mcnc.org/mumps.html>.



(a)



(b)

Fig. 4. Fabricated micromechanical tilt-mirror array: (a) top view and (b) perspective view.

by zig-zag torsion bars which allow them to rotate around a tilt axis defined by a pair of support points at either end. Each device has two electrical contacts leading to electrodes under the tilt plates, while the mirror plates are connected to a common ground. When the voltage on one of the contacts is increased (and the other contact grounded), each mirror goes through a regime of continuously increasing analog deflection. However, the switch is designed to use digital positions. At about 20 V applied the mirror snaps down to contact the substrate, producing a repeatable deflection angle of  $5^\circ$  relative to the substrate surface. The edges of the mirror plate have landing tips to reduce the contact area and therefore the probability of stiction (semipermanent bonding of the mirror edge with the substrate). At still higher drive voltages (about 30 V), the devices apparently snap down into full contact with the substrate, becoming parallel to the substrate surface.

The mirrors were operated with an ac drive voltage to avoid electrostatic charging. When operated with a dc voltage for several seconds to minutes (depending on humidity), switching would lag the drive voltage by longer and longer until the devices eventually stopped. This apparently arises from charg-

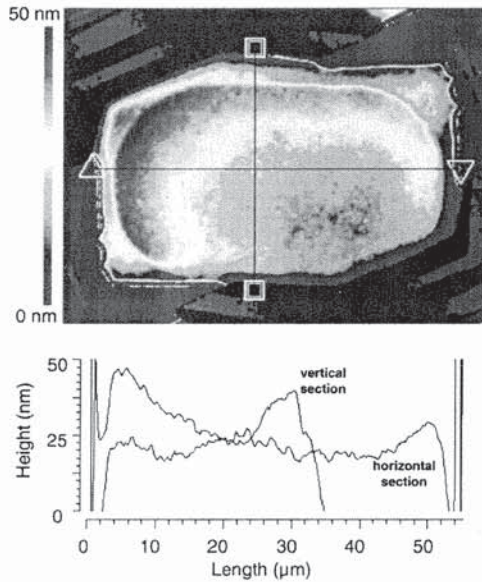
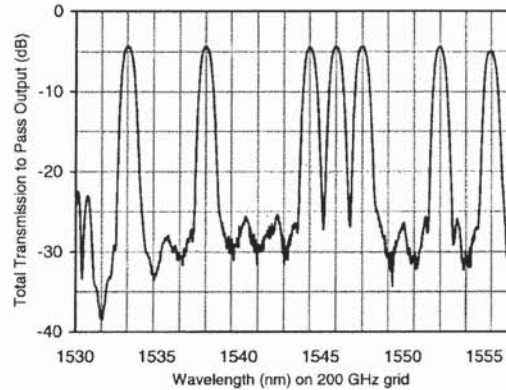


Fig. 5. Surface profile of individual micromechanical tilt-mirror.

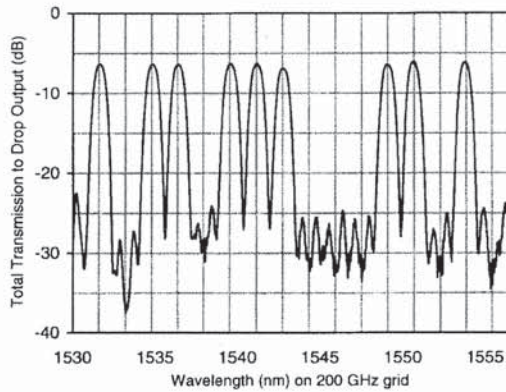
ing of the exposed dielectric (silicon nitride) surface beneath the mirror electrode. After the contacts were grounded to dissipate the accumulated shielding charge the devices would function normally again. However, these charging effects were completely eliminated by replacing the dc drive voltage with a high frequency ac drive voltage. The electrostatic switch is insensitive to the sign of the drive voltage. When the drive oscillates around zero at a frequency much larger than the device's mechanical resonant frequency, the charging is proportional to the averaged voltage level (which is zero), while the deflection is proportional to the root mean square voltage. We verified this experimentally, and found that a sinusoidal drive signal oscillating at 300 kHz with a peak-to-peak amplitude of 80 V produced reliable switching for extended operation times.

The current MUMP's process is not optimized for optical MEMS applications. The best mirrors available in the standard process use a 0.5- $\mu\text{m}$  thick gold layer principally intended for wire bond pads. This gold layer has residual stress and can cause curvature of the released polysilicon plates, especially over wide thermal excursions. We used an interferometric surface profilometer to characterize our devices. The original devices, fabricated entirely within the MUMP's process, had a 0.17  $\mu\text{m}$  sag across the full 57  $\mu\text{m}$  width of the tilt-mirror plate. This can cause the angle of the reflected beam to vary by as much as 0.7° depending on where the mirror is illuminated, an angle large enough to potentially reduce switching contrast.

For our mirrors, we deposited 3 nm of chrome, followed by 50 nm of gold directly onto the top polysilicon layer of the MUMPS die. This composition should produce similar reflectivity to the original 500 nm metal layer, but result in significantly lower stress. Fig. 5 shows the mirror surface profile. The top is a false-color map of a single mirror, indicating



(a)



(b)

Fig. 6. (a) PASS and (b) DROP transmission of ASE input dropping eight of 16 channels.

two cross sections shown below. With no voltage applied, the mirror is very slightly tilted relative to the substrate, but the curvature of the cross sections indicate that the stress-induced sag has been reduced to 0.02  $\mu\text{m}$  (20 nm) across the full 57  $\mu\text{m}$  aperture. This produces less than  $\lambda/20$  phase variation in the reflected optical wavefront, a flatness comparable to a polished glass mirror.

### III. PERFORMANCE

Test results for the assembled and aligned WAD switch are shown in Figs. 6–11. The total fiber-to-fiber insertion loss was approximately 5 dB for the PASS output and 8 dB for the DROP output, including the circulators. The difference between the two states comes from the slightly larger than optimal mirror switching angle (we chose to align the optical system to minimize PASS losses). The polarization dependent loss ranged from 0.1 to 0.2 dB. About 1.8 dB of the loss comes from two passes through the circulators; 1.7 dB from two passes through the grating, and the remaining 1.5 dB comes from residual surface reflections and aberrations. Comparing the 5 dB loss to the 4.6 dB loss obtained using a simple gold

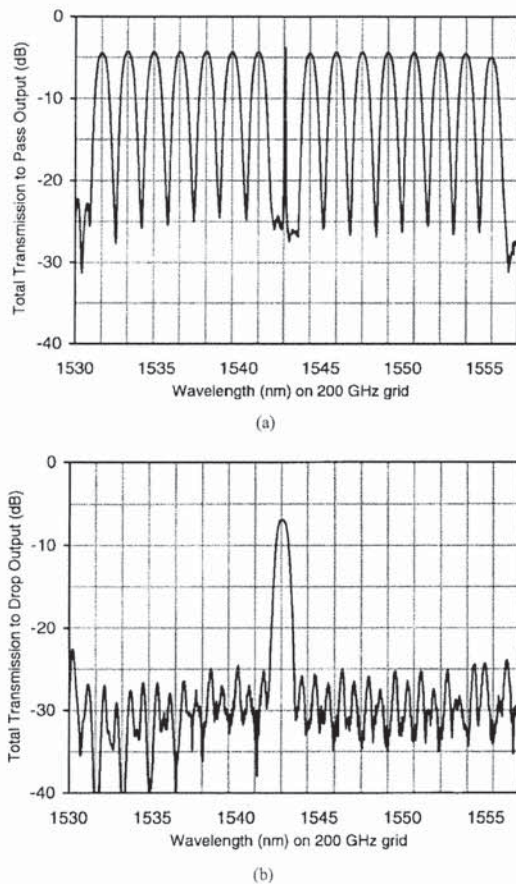


Fig. 7. (a) PASS and (b) DROP transmission of ASE input when channel 8 is dropped and replaced by light from a tunable laser.

mirror, we see that the surface quality of the micro mirror devices is good for this type of micromechanical structure.

Broad spectrum measurements of switch transmission were performed using an Erbium-doped fiber ASE (amplified spontaneous emission) source. Fig. 6(a) shows the PASS and Fig. 6(b) shows the DROP output with 9 of the 16 switches set to drop. The original source nonuniformity has been subtracted to show absolute transmission. The 3 dB roll off in both PASS and DROP passbands occurs at a full width of 0.7 nm, as compared to the 1.59 nm pitch between channels. These passbands are created by the nonreflective spaces between the mirrors. The slightly flattened Gaussian shape of the passbands can be calculated by convolving the optical spot size at the device plane (full width at half maximum of about  $14\ \mu\text{m}$ ) with the (roughly)  $30\ \mu\text{m}$  wide mirror aperture. Fig. 7 illustrates single channel drop-and-replace: channel 8 is dropped from Fig. 7(a) the pass output to Fig. 7(b) the drop output, and replaced by a narrow line width signal from a tunable laser source connected to the add port.

The switch is designed to operate on the ITU frequency grid with 200 GHz wavelength channel spacing. We used a

wavelength tunable source and polarization dependent loss meter to measure the switching contrast at the center of each of the 16 wavelength channels and each of the four possible switch states. Fig. 8 shows a bar graph of the results. The switching contrast for IN to PASS, or IN to DROP and ADD to PASS states is at least 32 dB, and ranges as high as 47 dB. Signals are never routed from ADD to DROP. The extinction between ADD and DROP terminals was at least 36 dB, in either direction. These measurements were taken when switching a single channel. The change in crosstalk created by switching the adjacent channels, and by switching various combinations of the other 15 channels, was measured to be below 1 dB.

Broad spectrum measurements of the switching contrast were made by using the ASE source and spectrum analyzer to store the "ON" transmission, then divide by the "OFF" transmission. The result is plotted in Fig. 9 for switching from the IN port to both the PASS and DROP outputs. The switching contrast measured using a laser tuned to each of the 16 channels (shown in Fig. 8) is also plotted, to verify this result. The switching contrast is sharply peaked at the center of the passband, where the optical spot on the tilt-mirror switch is entirely reflected. As the wavelength is shifted toward the edge of the passband, some of the input spot falls on to the mirror edge and is scattered into a wide angular range. A portion of the scattered light couples to the opposite switch output, resulting in crosstalk. Defining the operating passband as the spectral width which maintains a 30 dB or higher switching contrast, we see that the PASS output has a 0.57 nm average (0.40 nm minimum) operating passband, and the DROP output has a 0.34 nm average (0.28 nm minimum) operating passband.

The WAD switching response is shown in Fig. 10. The vertical lines, separated by  $20\ \mu\text{s}$ , indicate a switching time which is significantly faster the millisecond response typically required in SONET ring recovery.

This switch was intended as a first proof-of-principle demonstration, as opposed to a preproduction prototype, so reliability was not tested in any systematic manner. However, the switch operated as part of a week-long technology demonstration in a semi-enclosed (covered but not air-conditioned) temporary pavilion. The switch functioned normally, without adjustment, despite the wide swings in temperature and humidity characteristic of a New Jersey summer.

Finally, the ability of the switch to transmit data on multiple wavelengths was tested using the arrangement shown in Fig. 11. The test used two eight wavelength multifrequency lasers with 200 GHz pitch between wavelengths [13]. The two lasers were temperature tuned so that the wavelengths aligned exactly, creating the worst possible case for coherent crosstalk noise. Independent data streams from two 622 Mb/s (OC-3) word generators was applied to all wavelengths of each laser with two external electroabsorption modulators. The input signals were connected to the IN and ADD ports of the switch, and the transmitted PASS and DROP outputs were converted to electrical signals and fed into a GHz oscilloscope triggered by either of the word generators. The transmission eyes for the data are shown in the lower half of Fig. 11; at

# Explore Litigation Insights

Docket Alarm provides insights to develop a more informed litigation strategy and the peace of mind of knowing you're on top of things.

## Real-Time Litigation Alerts



Keep your litigation team up-to-date with **real-time alerts** and advanced team management tools built for the enterprise, all while greatly reducing PACER spend.

Our comprehensive service means we can handle Federal, State, and Administrative courts across the country.

## Advanced Docket Research



With over 230 million records, Docket Alarm's cloud-native docket research platform finds what other services can't. Coverage includes Federal, State, plus PTAB, TTAB, ITC and NLRB decisions, all in one place.

Identify arguments that have been successful in the past with full text, pinpoint searching. Link to case law cited within any court document via Fastcase.

## Analytics At Your Fingertips



Learn what happened the last time a particular judge, opposing counsel or company faced cases similar to yours.

Advanced out-of-the-box PTAB and TTAB analytics are always at your fingertips.

## API

Docket Alarm offers a powerful API (application programming interface) to developers that want to integrate case filings into their apps.

## LAW FIRMS

Build custom dashboards for your attorneys and clients with live data direct from the court.

Automate many repetitive legal tasks like conflict checks, document management, and marketing.

## FINANCIAL INSTITUTIONS

Litigation and bankruptcy checks for companies and debtors.

## E-DISCOVERY AND LEGAL VENDORS

Sync your system to PACER to automate legal marketing.